# Stable Dimeric Aromatic Cation–Radicals. Structural and Spectral Characterization of Through-Space Charge Delocalization

Jay K. Kochi,* Rajendra Rathore, and Pierre Le Maguères

*Department of Chemistry, University of Houston, Houston, Texas 77204-5641*

*jkochi@pop.uh.edu*

The spontaneous assembly of aromatic cation–radicals ($D^{+\bullet}$) with the parent donor (D) to afford the paramagnetic dimer $(D)_2^{+\bullet}$ is accompanied by a dramatic color change. For example, spectral (UV–vis and ESR) and X-ray crystal structure analyses establish the molecular association of octamethylbiphenylene cation–radical with its neutral counterpart to produce the mixed-valence or dimeric cation–radical in which the positive charge is completely delocalized over both aromatic moieties. The use of the sterically hindered cation–radicals confirms the new spectral or charge-resonance (CR) band to result in dimeric cation–radicals in which the intermolecular separation occurs at an optimum distance allowed by van der Waals contacts. The striking similarities between the classical donor/acceptor (EDA) complexes and the dimeric cation–radicals $(D)_2^{+\bullet}$ (both in terms of the geometrical requirement as well as the appearance of new absorption bands) suggest that the latter can be considered as particular examples of Mulliken's charge-transfer complexes in which the positive charge is completely (equally) delocalized over both donor (D) and acceptor ($D^{+\bullet}$).

## Introduction

The one-electron oxidation of a variety of aromatic donors (D) generates the paramagnetic cation–radicals which spontaneously associate with their neutral counterparts to form stabilized dimeric cation–radicals[1], i.e.

$$D^{+\bullet} + D \rightleftharpoons (D,D)^{+\bullet} \qquad (1)$$

On the basis of ESR spectroscopic data, Lewis and Singer[2] were first to postulate a sandwich-like structure for the naphthalene dimeric cation–radical, and they considered the unpaired electron to be equally distributed between the two naphthalene moieties. Brocklehurst and Rodgers[3,4] later examined the electronic absorption spectra of various aromatic cation–radicals by $\gamma$ irradiation in frozen glasses and by pulse radiolysis. They observed new broad absorption bands in the near-IR region characteristic of the dimeric cation–radicals, in addition to the (shifted and distorted) absorption bands of the monomeric cation–radicals in the visible region. These broad NIR absorption bands were termed "charge-resonance" bands and ascribed to charge–resonance transitions within the dimeric cation–radicals. Over the years, several though scattered examples of such self-assembled cation–radical dimers have been character-

ized spectroscopically,[5–7] and as a common feature, they all invariably show a diagnostic absorption band in the NIR region (see Table 1 for representative examples).

Stable dimeric cation–radicals are of fundamental importance to organic materials science since they constitute the smallest intermolecular units that carry a delocalized positive charge and thus provide the basis for the (photo)conductivity, ferromagnetism, etc., in various organic materials.[8–10] Several dimeric cation–radicals such as naphthalene and a few of its derivatives have been characterized by X-ray crystallography.[1,8] However,

(1) Fritz, H. P.; Gebauer, H.; Friedrich, P.; Ecker, P.; Artes, R.; Schubert, U. *Z. Naturforsch.* **1978**, *33b*, 498.

(2) (a) Lewis, L. C.; and Singer, L. S. *Chem. Phys.* **1965**, *43*, 2712. The hyperfine splittings in the dimeric radical cation are as follows: 2.77 (8H) and 1.03 (8H) whereas they are 5.86 (4H) and 1.66 (4H) in the monomeric radical cation (Erickson, R.; Benetis, N. P.; Lund, A.; Lindgren, M. *J. Phys. Chem.* **1997**, *101*, 2390. (b) Also see Howarth, O. W.; Fraenkel, G. K. *J. Am. Chem. Soc.* **1966**, *88*, 4514.

(3) (a) Badger; B., Brocklehurst, B. *Trans. Faraday Soc.* **1969**, *65*, 2582 and 2588. (b) Badger, B.; Brocklehurst, B. *Trans. Faraday Soc.* **1970**, *66*, 2939. (c) Badger, B.; Brocklehurst, B. *Nature (London)* **1968**, *219*, 263.

(4) Rodgers, M. A. J. *J. Chem. Soc., Faraday Trans. 1* **1972**, *68*, 1278.

(5) (a) Howarth, O. W.; Fraenkel, G. K. *J. Chem. Phys.* **1970**, *52*, 6258. (b) Torrance, J. B.; Scott, B. A.; Kaufman, F. B.; Seiden, P. E. *Phys. Rev. B* **1979**, *19*, 730. (c) Inokuchi, Y.; Naitoh, Y.; Ohashi, K.; Saito, K. I.; Yoshihara, K.; Nishi, N. *Chem. Phys. Lett.* **1997**, *269*, 298. (d) Takamuku, S.; Komitsu, S.; Toki, S. *Radiat. Phys. Chem.* **1989**, *34*, 553. Also see (e) Tsujii, Y.; Tsuchida, A.; Ito, S.; Yamamoto, M. *Macromolecules* **1991**, *24,* 4061.

(6) (a) Masnovi, J. M.; Kochi, J. K. *J. Phys. Chem.* **1987**, *91*, 1878. (b) Masnovi, J. M.; Kochi, J. K. *J. Am. Chem. Soc.* **1985**, *107*, 6781. (c) Gerson, F.; Kaupp, G.; Ohya-Nishiguchi, O. *Angew. Chem., Int. Ed. Engl.* **1977**, *16*, 657.

(7) The qualitative MO energy diagram for the dimeric cation–radical is
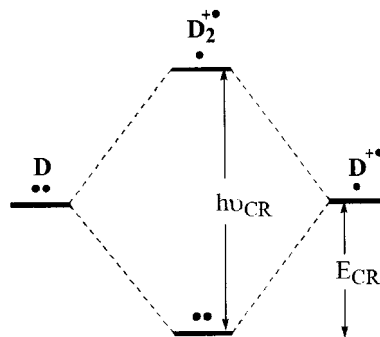
in which the origins of the stabilization energy ($E_{CR}$) and the charge-resonance spectral band ($h\nu_{CR}$) are as indicated. Compare: Bally, T.; Roth, K.; Straub, R. *J. Am. Chem. Soc.* **1988**, *110*, 1639.

**Table 1. UV-vis Spectra of Various Dimeric Aromatic Cation−Radicals**

| | | dimeric cation−radical (ArH)$_2{}^{+\cdot}$ | | |
| | | UV−vis | CR band[a] | |
| | donor (ArH) | $\lambda$ (nm) | $\lambda_{CR}$ (nm) | ref |
|---|---|---|---|---|
| **BZ** | benzene | 555 | 920 | b |
| **HMB** | hexamethylbenzene | 476, 508 | 1351 | b |
| **DTP** | 1,3-*p*-tolylpropane | 460 | >800 | c |
| **NAP** | naphthalene | 575 | 1050 | b |
| **AN** | anthracene | 680 | >900 | d |
| **PYR** | pyrene | 500 | 1400 | b |

[a] Charge-resonance band. [b] Taken from ref 3a. [c] Taken from ref 6. [d] Taken from ref 7.

there is no example extant in the literature in which the monomer and the dimer cation−radicals from the same aromatic system were isolated and structurally characterized. We have recently reported the isolation and X-ray crystallographic characterization of dimeric cation−radical of octamethylbiphenylene (**OMB**) using triethyloxonium hexachloroantimonate as a one-electron oxidant.[11]

In the present study, we describe the successful isolation and X-ray crystallographic characterization of monomeric **OMB**$^{+\cdot}$ cation−radical salt which provides the basis for a direct structural comparison of monomeric and sandwiched-dimeric cation−radicals. Moreover, the preparation of highly pure monomeric **OMB**$^{+\cdot}$ cation−radical allows us to directly monitor the dimerization process (see eq 1) by UV−vis and ESR spectroscopy. By analogy to the charge-transfer absorptions of diamagnetic electron donor/acceptor (EDA) complexes described by Mulliken theory,[12] the charge-resonance bands in paramagnetic cation−radical dimers are ascribed to charge delocalization between the neutral (donor) and the oxidized (acceptor) arene moieties due to strong ($\pi,\pi$)-orbital overlap.[3] In a recent study, we have shown that optimum electronic coupling in EDA assemblies requires a cofacial arrangement of donor and acceptor with an interplanar separation of ∼3.5 Å.[13a] [Similar geometrical requirements have also been found for donor/acceptor encounter (excited state) complexes and excimers.][13b] Accordingly, we will

also employ sterically hindered and unhindered aromatic compounds in this study to probe the geometrical requirements for the orbital overlap (and charge delocalization) in dimeric cation−radicals. Moreover, a detailed spectroscopic and structural comparison of the association of an aromatic donor with its cation−radical (i.e., to form self-assembled dimeric cation−radical) and with a variety of other cationic and neutral electron acceptors (i.e., to form donor−acceptor complexes) will form the basis for the discussion of charge-resonance (CR) transitions and charge-transfer (CT) transitions in terms of degree of electronic delocalization.

## Results and Discussion

**A. Spectral and Structural Comparison of Monomeric and Dimeric Octamethylbiphenylene Cation−Radicals.** To delineate the intermolecular dimerization process in eq 1 leading to the dimeric cation−radical, we initially employ octamethylbiphenylene **OMB**$^{+\cdot}$ cation-radical salt owing to its high stability under ambient conditions as follows.

**1. Preparation of Monomeric Octamethybiphenylene Cation−Radical Salt.** A solution of **OMB** in dichloromethane was added to a slurry of triethyloxonium hexachloroantimonate salt (under an argon atmosphere) at −20 °C. Upon continued stirring (4 h), the mixture turned deep blue, and the quantitative (UV−vis) spectral analysis of the brightly colored solution showed a characteristic spectrum with an absorption band at $\lambda_{max}$ = 600 nm ($\epsilon_{600}$ = 12000 M$^{-1}$ cm$^{-1}$) and a shoulder at 550 nm (see Figure 1A) due to the formation of **OMB**$^{+\cdot}$, i.e.
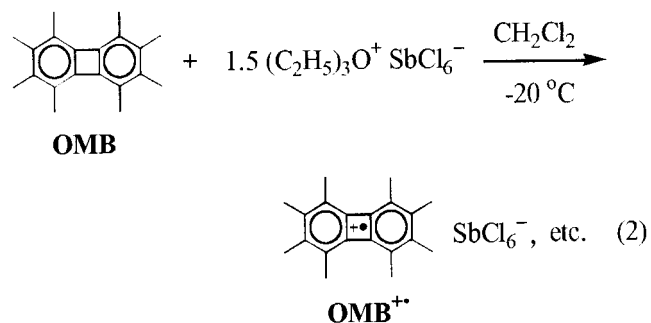


The highly colored solution was cooled to −50 °C and prechilled toluene was added. The dark-blue precipitate of **OMB**$^{+\cdot}$SbCl$_6{}^-$ thus formed was filtered under an argon atmosphere and dried in vacuo (0.88 mmol). The purity of the crystalline monomeric cation−radical salt was determined iodometrically and was found to be greater than 99% (see Experimental Section). After repeated attempts at recrystallization of the blue powder (by varying the solvents and the temperature), a good crop of single crystals of **OMB**$^{+\cdot}$SbCl$_6{}^-$ was finally obtained from a mixture of dichloromethane and hexane at −30 °C, and its molecular structure was unambiguously established by single-crystal structure analysis (vide infra).

**2. Spectral (UV−vis) Changes during the Dimerization of Octamethylbiphenylene Cation−Radical.** A blue solution of recrystallized **OMB**$^{+\cdot}$SbCl$_6{}^-$ in dichloromethane (at 25 °C) showed a characteristic absorption

(8) (a) Enkelmann, V. In *Advances in Chemistry Series*; Ebert, L. B., Ed.; American Chemical Society: Washington, D.C., 1987; Vol. 217, p 177 and references therein. (b) Kröhnke, C.; Enkelmann, V.; Wegner, G. *Angew. Chem., Int. Ed. Engl.* **1980**, *19*, 912. (c) Stenger-Smith, J. D.; Lenz, R. W.; Enkelmann, V.; Wegner, G. *Makromol. Chem.* **1992**, *193*, 575. (d) Ayllón, J. A.; Santos, I. C.; Henriques, R. T.; Almeida, M.; Lopes, E. B.; Morgado, J.; Alcácer, L.; Veiros, L. F.; Teresa Duarte, M. *J. Chem. Soc., Dalton Trans.* **1995**, 3543 and references therein. (e) Gama, V.; Henriques, R. T.; Bonfait, G.; Pereira, L. C.; Waerenborgh, J. C.; Santos, I. C.; Teresa Duarte, M.; Cabral, J. M. P.; Almeida, M. *Inorg. Chem.* **1992**, *31*, 2598. (f) Keller, H.; Nöthe, D.; Pritzkow, H.; Wehe, D.; Werner, M.; Koch, P.; Schweitzer, D. *Mol. Cryst. Liq. Cryst.* **1980**, *62*, 181.

(9) (a) Jerome, D.; Ribault, M.; Bechgaard, K. *J. Phys. Lett.* **1980**, L95. (b) Williams, J. M.; Kini, A. M.; Wang, H. H.; Carlson, K. D.; Geiser, U.; Montgomery, L. K.; Pyrka, G. J.; Watkins, D. M.; Kommers, J. M.; Boryschuk, S. J.; Crouch, A. V. S.; Kwok, W. K.; Schriber, J. E.; Overmeyer, D. L.; Jung, D.; Whangbo, M. H. *Inorg. Chem.* **1990**, *29*, 3272. (c) Williams, J. M.; Ferraro, J. R.; Thorn, R. J.; Carlson, K. D.; Geiser, U.; Wang, H. H.; Kini, A. M.; Whangbo, M. H. *Organic Superconductors. Synthesis, Structure, Properties and Theory*; Grimes, R. N., Ed.; Prentice Hall: Englewood Cliffs, NJ, 1992. (d) Kobayashi, H.; Tomita, H.; Naito, T.; Kobayashi, A.; Sakai, F.; Watanabe, T.; Cassoux, P. *J. Am. Chem. Soc.* **1996**, *118*, 368.

(10) For some recent examples of radical−cation dimerization processes, see: Hubler, P.; Heinze, J. *Ber. Bunsen. Phys. Chem./Chem. Phys.* **1988**, *102*, 1506, and references therein.

(11) Rathore R.; Kumar, A. S.; Lindeman, S. V.; Kochi, J. K. *J. Org. Chem.* **1998**, *63*, 5847.

(12) Mulliken, R. S. *J. Am. Chem. Soc.* **1952**, 74, 811. (b) Mulliken, R. S.; Person, W. B. *Molecular Complexes. A Lecture and Reprint Volume*; Wiley: New York, 1969. (c) See also Foster, R. *Organic Charge-Transfer Complexes*; Academic: New York, 1969.

(13) (a) Rathore, R.; Lindeman, S. V.; Kochi, J. K. *J. Am. Chem. Soc.* **1997**, *119*, 9393. (b) Rathore, R.; Hubig, S. M.; Kochi, J. K. *J. Am. Chem. Soc.* **1997**, *119*, 11468 and references therein.
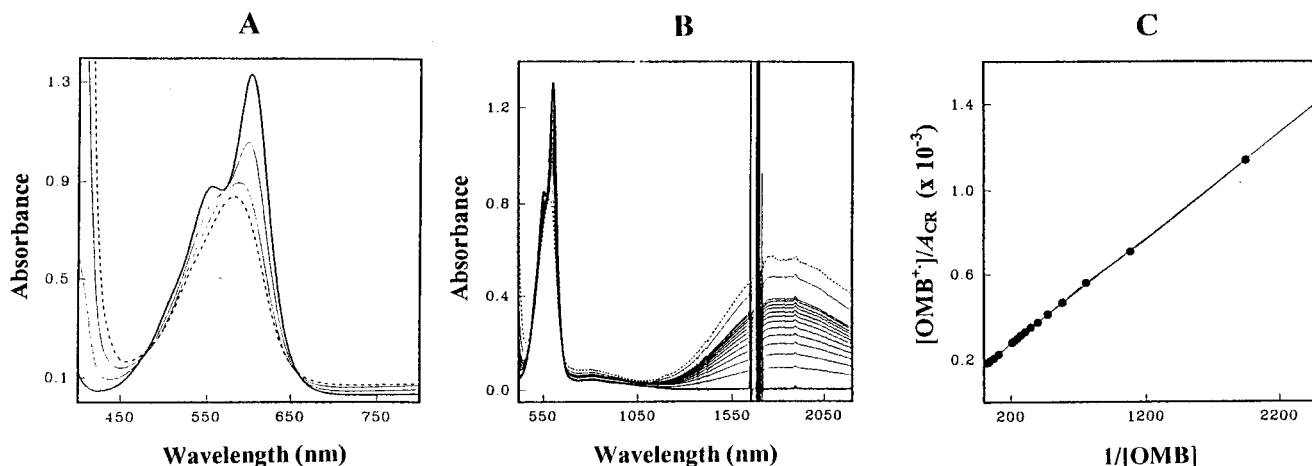
**Figure 1.** UV−vis spectral changes during formation of dimeric $(OMB)_2^{+\bullet}$: (A) Slow cooling from room temperature to −78 °C of a mixture of monomeric $OMB^{+\bullet}SbCl_6^-$ cation−radical salt with 2 to 3 equiv of neutral **OMB** in dichloromethane. (B) Incremental addition of neutral **OMB** to a dichloromethane solution of monomeric $OMB^{+\bullet}SbCl_6^-$ cation−radical salt at room temperature. (C) Benesi-Hildebrand plot for the experiment in B.

spectrum with a twin band that remained unchanged upon cooling the solution to −78 °C. When the blue solution at room temperature was mixed with 2 to 3 equiv of neutral **OMB** and slowly cooled to −78 °C, the UV− vis spectral changes in Figure 1A showed a progressive merging of the twin absorption band to a single Gaussian band (vide infra). [Also note that the color of the solution changed from bright-blue to light-purple upon cooling to −78 °C.] In another experiment, the absorption spectra of the blue solution were recorded from 300 to 2500 nm at 25 °C upon incremental addition of neutral octamethylbiphenylene at 25 °C. The spectral changes in Figure 1B showed a similar merging of the twin absorption band ($\lambda_{max}$ = 600 and 550 nm) to a Gaussian band ($\lambda_{max}$ = 570 nm), but also the growth of a new broad absorption band in the NIR region at $\lambda_{max}$ = 1850 nm. This characteristic NIR absorption band was ascribed to the formation of dimeric $(OMB)_2^{+\bullet}$ cation−radical, i.e.

$$OMB^{+\bullet} \;+\; OMB \;\; \underset{}{\overset{K_{dimer}}{\rightleftharpoons}} \;\; (OMB)_2^{+\bullet} \tag{3}$$

in which the absorption band derives from charge-resonance transitions.

For the quantitative analysis of the formation of dimeric $(OMB)_2^{+\bullet}$ cation−radical in solution, we employed the Benesi−Hildebrand (spectrophotometric) procedure[14] (which is generally utilized for the quantification of diamagnetic electron donor−acceptor associations) in which the absorbance changes in Figure 1B were treated according to eq 4, i.e.

$$\frac{[OMB^{+\bullet}]}{A_{CR}} \;=\; \frac{1}{\varepsilon_{CR}} \;+\; \frac{1}{K_{dimer}\varepsilon_{CR}} \;\frac{1}{[OMB]} \tag{4}$$

where $A_{CR}$ is the absorbance and $\epsilon_{CR}$ is the molar extinction coefficient of the charge-resonance band at the monitoring wavelength. Thus a plot of $[OMB^{+\bullet}]/A_{1850}$ vs the reciprocal concentration of added neutral octamethylbiphenylene **OMB** was linear, and the least-squares fit produced a correlation coefficient greater than 0.999 in

Figure 1C. From the slope $[K_{dimer}\,\epsilon_{CR}]^{-1}$ and the intercept $[\epsilon_{CR}]^{-1}$, the values of the dimerization constant and the extinction coefficient of the charge-resonance band were readily extracted as $K_{dimer}$ = 350 M$^{-1}$ and $\epsilon_{1850}$ = 5700 M$^{-1}$ cm$^{-1}$, respectively. Note that the same extinction coefficient ($\epsilon_{1850}$ = 5670) was obtained by the quantitative comparison of the charge-resonance band [from the final spectrum (- - - -) in Figure 1B] with the local band of monomer $OMB^{+\bullet}$ cation−radical with an extinction coefficient $\epsilon_{600}$ = 12020 M$^{-1}$ cm$^{-1}$ [from the first spectrum (—) in Figure 1B]. It is also noteworthy that the dimerization equilibrium constant ($K_{dimer}$) for octamethylbiphenylene cation−radical is of the same order of magnitude as that obtained for hexamethylbenzene, naphthalene, and pyrene cation−radicals by the pulse-radiolytic method.[4a]

**3. ESR Spectra of the Monomeric and Dimeric Octamethylbiphenylene Cation−Radical.** The well-resolved ESR spectrum in Figure 2 obtained in dilute solution of monomeric $OMB^{+\bullet}$ cation−radical at 25 °C showed at least 13 lines with a hyperfine splitting of $a_H$ = 4.5 G ($g$-value = 2.0023). The hyperfine splitting corresponds to 12 equivalent protons, and it was successfully simulated using the WinSIM software[15] (see Figure 2). This ESR spectrum remained unchanged upon cooling the solution to −80 °C.

When the same solution of $OMB^{+\bullet}$ cation−radical, in the presence of excess (3 equiv) neutral **OMB** at 25 °C (otherwise under identical conditions), was subjected to ESR analysis, it produced a broad unresolved signal which could be readily resolved at −80 °C with at least 15 lines (see Figure 2). The well-matching computer simulation of this spectrum is also shown in Figure 2. Interestingly, the 15-line (resolved) spectrum showed a hyperfine splitting of $a_H$ = 2.3 G which arises from 24 equivalent protons, each having approximately one-half the hyperfine-splitting constant of the protons from the monomeric $OMB^{+\bullet}$ cation−radical, and thus this ESR spectrum was readily assigned to dimeric octamethylbiphenylene cation−radical.[2]

(14) (a) Benesi, H. A.; Hildebrand, J. J. *J. Am. Chem. Soc.* **1949**, *71*, 2703. (b) Foster, R. *Molecular Complexes*; Crane, Russak & Co.: New York, 1974, Vol. 2.

(15) P.E.S.T WinSIM software for EPR simulations for MS−Windows NT, 95, Version: 0.96; Public EPR Software Tools, National Institute of Environmental Health Sciences.

Experimental          Calculated
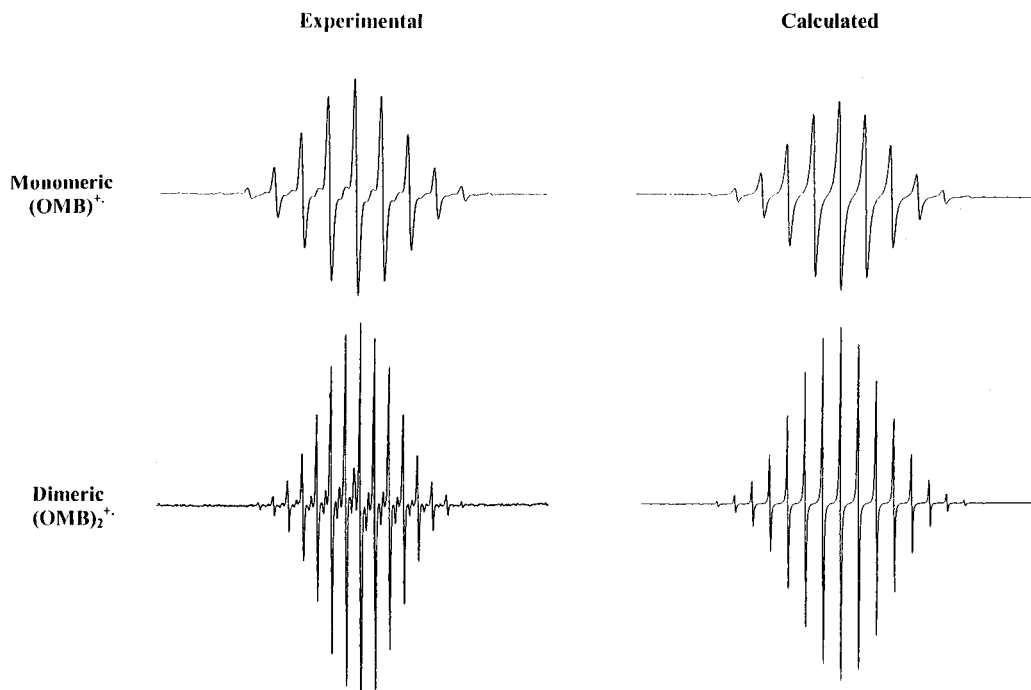


**Figure 2.** Experimental ESR spectra of monomeric **OMB**[+•]SbCl$_6$[−] and dimeric (**OMB**)$_2$[+•]SbCl$_6$[−] cation−radical salts in dichloromethane at room temperature and comparison with their calculated spectra.

## 4. Structural Comparison of Neutral Octamethylbiphenylene with Its Monomeric and Dimeric Cation−Radical Salts.

The successful isolation of single-crystals of both octamethylbiphenylene cation−radical monomer **OMB**[+•] and dimer (**OMB**)$_2$[+•] allowed their molecular structures to be directly compared to each other and to that of the neutral **OMB** by X-ray diffraction analysis. For convenience, the equivalent bonds in octamethylbiphenylene are denoted by lower-case bold letters **a** to **e** (see structure **A**).

**Changes in Bond Lengths.** The molecular structure of neutral octamethylbiphenylene[16] shows a considerable bond alternation due to the antiaromatic nature of the cyclobutane ring.[17] For example, the C−C bond **a** in the cyclobutane ring of neutral **OMB** is considerably longer (1.522 Å) than the C$_{ar}$−C$_{ar}$ bond length (1.490 Å) found in various biphenyls.[18] Moreover, the bonds **b** and **d** are significantly elongated as compared to the bonds **c** and **e** in the two benzene rings (see Table 2). Such a bond alternation in neutral **OMB** can be represented by structure **A** as the most contributing resonance form, i.e.,

**A.**
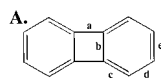


In the monomeric cation−radical **OMB**[+•], the removal of an electron resulted in a considerable shortening (5 pm) of bonds **a** (1.475 Å) in the cyclobutane ring and

**Table 2. Average Lengths for the Equivalent Bonds within the Phenyl Rings of OMB Moiety in the Neutral Donor and the Monomeric and the Dimeric Cation−Radicals**[a]

| intraring C−C bond | neutral[a] | (OMB)$_2$[+• b] | OMB[+• c] |
|---|---|---|---|
| **a** | 1.522(5) | 1.495(5) | 1.475(4) |
| | | **−2.7 pm** | **−4.7 pm** |
| **b** | 1.418(5) | 1.432(5) | 1.450(4) |
| | | **+1.4 pm** | **+3.2 pm** |
| **c** | 1.365(5) | 1.380(5) | 1.386(4) |
| | | **+1.5 pm** | **+2.1 pm** |
| **d** | 1.435(5) | 1.424(5) | 1.416(4) |
| | | **−1.1 pm** | **−1.9 pm** |
| **e** | 1.391(5) | 1.420(5) | 1.433(4) |
| | | **+2.9 pm** | **+4.2 pm** |

[a] The bold numbers indicate the bond length changes relative to the neutral donor. [a] Taken frm ref 16. [b] Taken from ref 11. [c] This work.

lengthening of bonds **b** (3 pm) and **e** (4 pm) in the aromatic rings. Interestingly, the adjacent bonds **c** and **d** were elongated and contracted, respectively, by about 2 pm (see Table 2). This observed variation in lengths of the relevant bonds **a**−**e** in **OMB**[+•] suggests a significant contribution from an alternate canonical structure **B**, i.e.,

**B.**



OMB          OMB[+•]
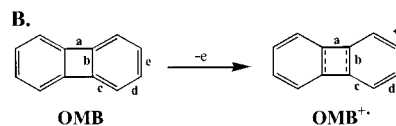
Furthermore, a comparison of the alternating contraction and elongation of bonds **a**, **b**, **d**, and **e** in dimeric (**OMB**)$_2$[+•] cation−radical with neutral **OMB** showed that the changes in various bond lengths were approximately one-half of those in the monomeric **OMB**[+•] cation−radical (see Table 2). In fact, the structural comparison between monomeric and dimeric cation−radical reveals a complete

(16) Bowen Jones, J.; Brown, D. S.; Hales, A.; Massey, A. G. *Acta Crystallogr.* **1988**, *C44*, 1757.

(17) (a) Bowen Jones, J.; Brown, D. S.; Massey, A. G.; Slater, P. J. *J. Fluorine Chem.* **1986**, *31*, 75. (b) Fawcett, J. K.; Trotter, J. *Acta Crystallogr.* **1966**, *20*, 87. (c) Ali, M. A.; Coulson, C. A. *Tetrahedron* **1960**, *16*, 41. (d) Dewar, M. J. S.; Gleicher, G. J. *Tetrahedron* **1965**, *21*, 1817. (e) Randič, M.; Maksič, Z. B. *J. Am. Chem. Soc.* **1971**, *93*, 64.

(18) Allen, F. H.; Kennard, O.; Watson, D. G.; Brammer, L.; Orpen, A. G.; Taylor, R. *J. Chem. Soc., Perkin Trans. 2* **1987**, S1−S19.

**A**                                                         **B**
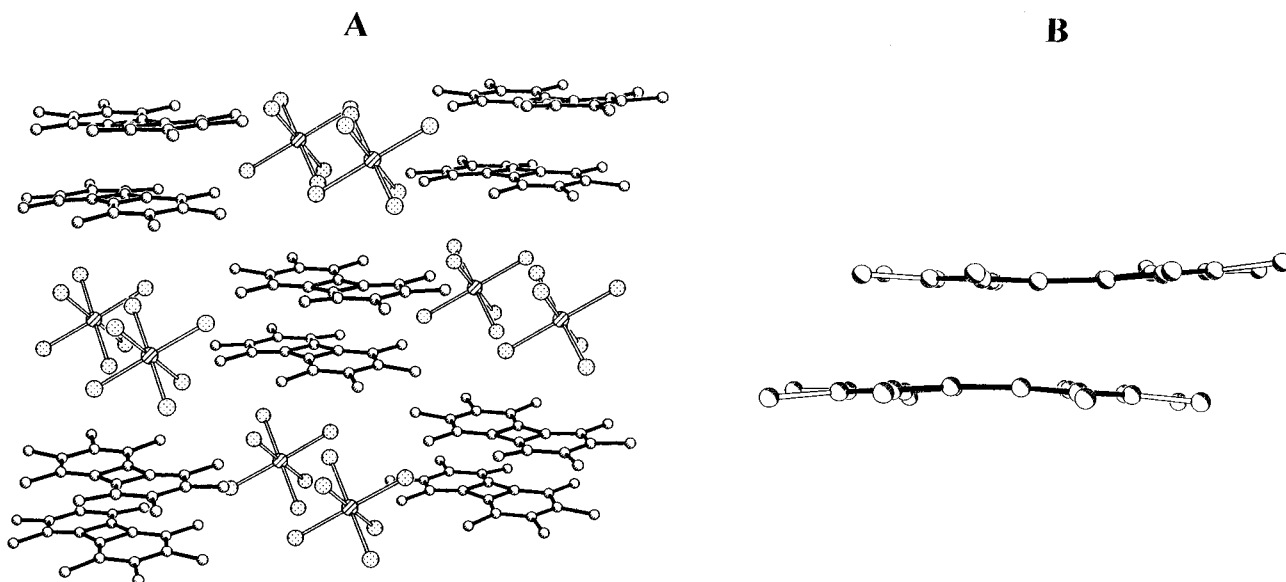


**Figure 3.** (A) Crystal structure representation of the cation–radical salt **OMB**$^{+•}$**SbCl**$_6^-$ showing the packing of pairs of cations with pairs of anions. (B) Side perspective view of a pair of **OMB**$^{+•}$ cation–radical in the SbCl$_6^-$ salt showing a concave shape.

delocalization of the positive (unity) charge over two **OMB** molecules within the dimeric cation–radical,[19] i.e.,

**C.**
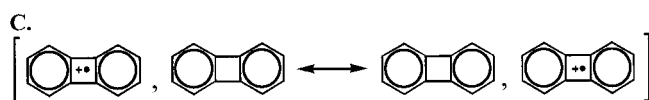


**Comparison of Molecular Packing.** In crystals, the monomeric **OMB**$^{+•}$**SbCl**$_6^-$ packed as pairs of cations separated by pairs of anions in infinite alternating stacks, as shown in Figure 3a. The close cofacial proximity (with an interplanar separation of 3.2 Å) of two identical **OMB**$^{+•}$ moieties induces a slight bending of the biphenylene ring system (see Figure 3b), the magnitude of which is gauged by the change in the intramolecular dihedral angle of $\delta = 6.3$ deg. between the mean planes of the benzene rings.[19b] For comparison, the octameth-

ylbiphenylene moieties in crystals of dimeric cation–radical were absolutely planar, and they were arranged in infinite (homosoric) stacks which were separated by intertwined columns of hexachloroantimonate anions and some triethyloxonium cations, as illustrated in Figure 4. Most importantly, the infinite stacks contained units of dimeric (**OMB**)$_2^{+•}$ as inferred from two distinct (and alternating) intermolecular (separations) distances of 3.41 and 3.54 Å between the planes of octamethylbiphenylene moieties. Indeed, the observed interplanar separation of 3.41 Å represents a tight van der Waals contact between the two identical octamethylbiphenylene moieties in the dimeric cation–radical as shown by the space filling representation **D** below.

**D.**
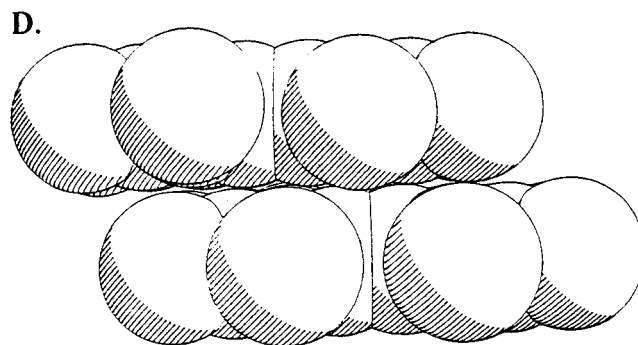


It is noteworthy that a mere van der Waals contact between two octamethylbiphenylene moieties in the dimeric cation–radical is sufficient for the charge transfer to occur which is confirmed by the observation of an intense charge-resonance absorption band at ∼1820 nm in the diffuse-reflectance UV–vis absorption spectrum of the crystalline dimeric (**OMB**)$_2^{+•}$.

**B. Steric Inhibition in the Formation of Dimeric Cation–Radicals.** As shown above in structure **D**, charge-resonance transitions (i.e., observation of the NIR absorption band) are observed at a distance of 3.41 Å in dimeric octamethylbiphenylene cation–radical. Thus, the question arises as to what the interplanar distance must be for the charge-resonance transitions to become neg-

---

(19) (a) In the centrosymmetric dimeric units (**OMB**)$_2^{+•}$, the two **OMB** moieties were crystallographically equivalent and thus indistinguishable. However, we inquired whether the two components of such dimeric cation–radicals are not distinguishable (a) because of the complete delocalization of the single positive charge (or a one-electron hole) or (b) merely due to a statistical disorder between neutral and cationic **OMB** (see structure **C**). To address this question, we obtained high-quality crystals of the dimeric cation–radical salt of structurally similar 1,2,3,4,5,6,7,8-octamethylanthracene (**OMA**) from a mixture of dichloromethane and hexane at −23 °C (for spectral details, see Table 3). The crystal structure analysis of the (**OMA**)$_2^{+•}$-SbCl$_6^-$ salt showed that it consists of well-separated centrosymmetric (**OMA**)$_2^{+•}$ dimers with an interplanar distance of 3.38 Å, in which the **OMA** moieties were completely indistinguishable. We next performed the rigid-body refinement procedure (Seiler, P.; Dunitz, J. D. *Acta Crystallogr. B.* **1979**, *B35*, 1068. Bürgi, M. B., Förtsch, M. *J. Mol. Struct.* **1999**, 485. Trueblood, K. N. In *Accurate Molecular Structures*; Domenicano, A., Margittai, I., Eds.; Oxford University Press: Cary, NC, 1992. Shomaker, V.; Trueblood, K. N. *Acta Crystallogr. B* **1968**, *B24*, 63.) to evaluate the temperature-dependence on the atomic vibrational parameters in **OMA** units on diffraction data collected at several temperatures (−150 °C, −90 °C and −30 °C, see Experimental Section). The thermal motion parameters for the **OMA** units conform well with a rigid body model (i.e., a discrepancy factor $R$(G) for the octamethylanthracene moiety is 2.97%, 3.02%, and 3.81% whereas for hexachloroantimonate anion it is 3.00%, 2.93%, and 2.45% at −30 °C, −90 °C, and −150 °C, respectively), and they are consistent with a completely delocalized structure. (b) The nature of the unusually close interplanar separation and bending of the biphenylene moieties in the crystal structure of **OMB**$^{•+}$ SbCl$_6^-$ (Figure 3) are under active investigation.
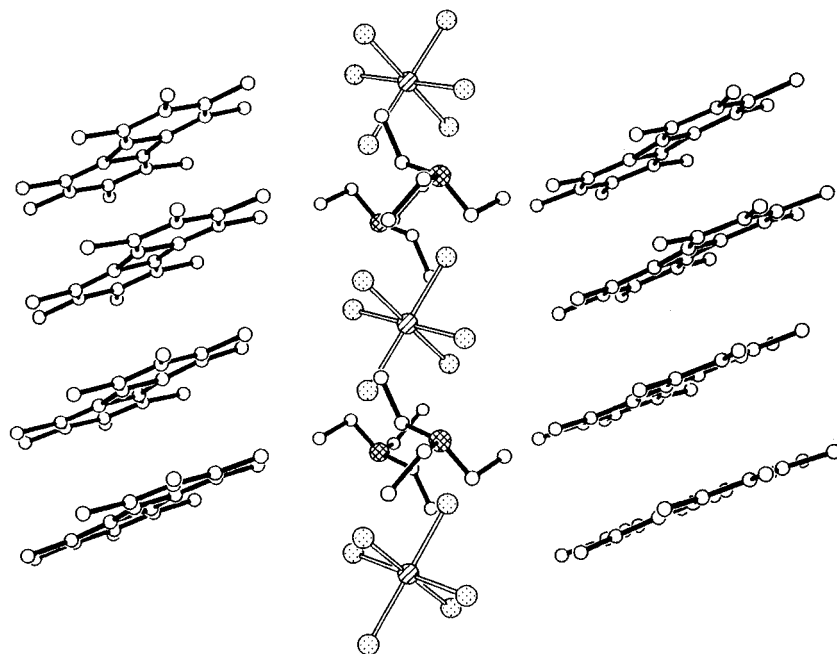
**Figure 4.** Crystal structure representation of the cation–radical salt (**OMB**)$_2^{+\bullet}$SbCl$_6^-$ showing the infinite stacks of octamethylbiphenylene cation–radicals separated by columns of hexachloroantimonate anions and some triethyloxonium cations.

**Chart 1**
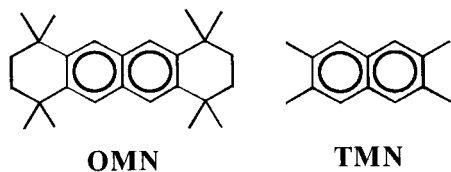


| | **OMN** | **TMN** |
|---|---|---|
| E$^o_{ox}$ (V *vs.* SCE) | 1.34 | 1.40 |

ligible. To address this question, we examine a sterically encumbered naphthalene derivative (**OMN**) and compare it with the sterically most accessible tetramethylnaphthalene (**TMN**) shown in Chart 1.

The oxidation of these naphthalene derivatives to the corresponding cation–radicals was carried out using nitrosonium hexachloroantimonate (NO$^+$SbCl$_6^-$) as follows.

**Hindered Naphthalene OMN.** A solution of the hindered naphthalene **OMN** in dichloromethane was added to crystalline NO$^+$SbCl$_6^-$ (under an argon atmosphere) at ~–10 °C. Continued stirring and removal of the gaseous nitric oxide (by bubbling argon through the dark solution) afforded a bright-blue solution (see Experimental Section). Spectral (UV–vis) analysis of the deep-blue solution showed a very characteristic absorption spectrum (see Figure 5) with absorption bands at $\lambda_{max}$ = 672 ($\epsilon_{672}$ = 9300 M$^{-1}$ cm$^{-1}$), 616, 503, and 396 nm. The absorption spectrum in Figure 5 was readily assigned to the monomeric **OMN**$^{+\bullet}$ cation–radical by comparison of its characteristic fine structure with that of parent naphthalene cation–radical (Table 3). [Note that the identical absorption spectrum of **OMN**$^{+\bullet}$ cation–radical with its characteristic fine structure was also obtained by an electrochemical oxidation in dichloromethane or by chemical oxidation with (C$_2$H$_5$)$_3$O$^+$SbCl$_6^-$ [11] and DDQ/CH$_3$SO$_3$H.[20]]

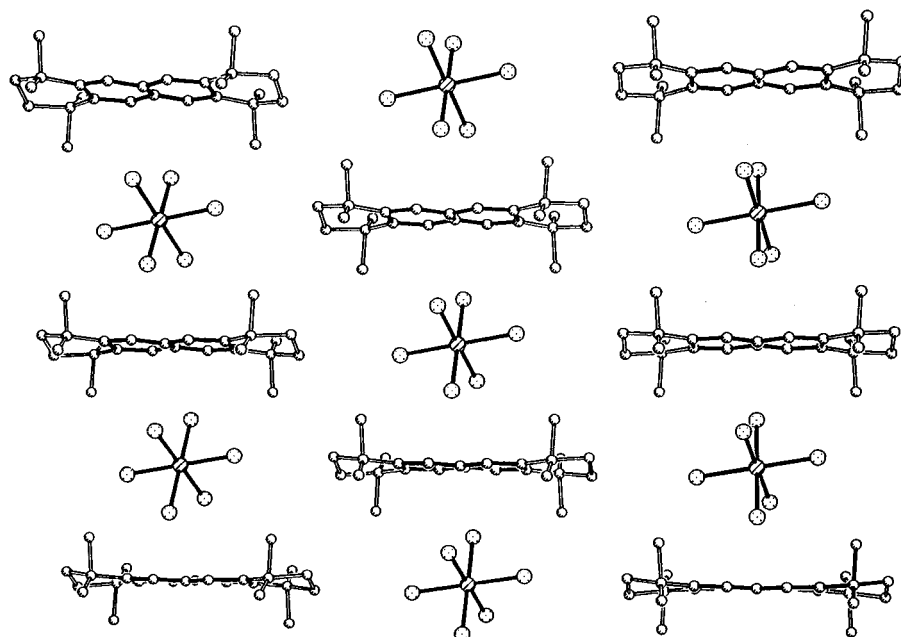(20) Rathore, R.; Kochi, J. K. *Acta Chem. Scand.* **1998**, *52*, 114.
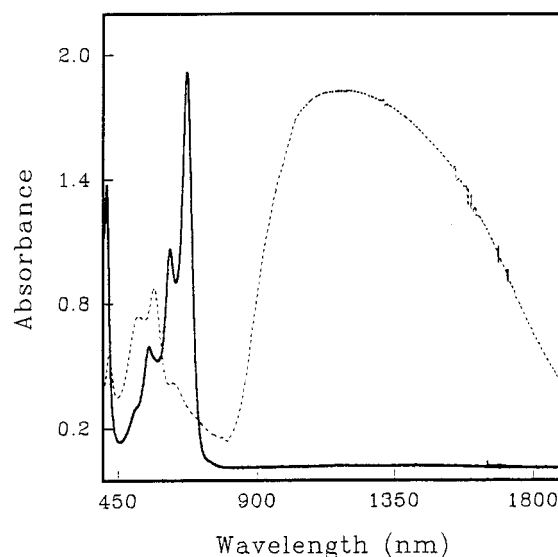


**Figure 5.** UV–vis absorption spectra of (—) a 0.0002 M solution of the cation–radical salt **OMN**$^{+\bullet}$SbCl$_6^-$ in dichloromethane at 0 °C showing the complete absence of absorption band in the NIR region and (·····) a 0.00013 M solution of the cation–radical salt (**TMN**)$_2^{+\bullet}$SbCl$_6^-$ in dichloromethane at –20 °C showing the presence of a NIR band at $\lambda_{max}$ = 1150 nm characteristic of the dimeric species.

In another experiment, a blue solution of **OMN**$^{+\bullet}$ was mixed with a 25 mM solution of neutral **OMN**, and the solution was cooled to –78 °C. The (UV–vis) spectral analysis of this solution again showed the characteristic spectrum of monomeric **OMN**$^{+\bullet}$ and a complete absence of any new absorption in the NIR region.

The **OMN**$^{+\bullet}$ cation–radical was readily isolated as a crystalline (dark-blue) hexachloroantimonate salt in quantitative yield by a slow diffusion of hexane into a dichloromethane solution of **OMN**$^{+\bullet}$SbCl$_6^-$ (see Experimental Section) and the purity of the salt (determined iodometrically) was measured to be greater than 99%.

**Figure 6.** Crystal structure of the cation−radical salt **OMN**$^{+}$·SbCl$_6^{-}$ showing isolated cation−radical units.

The isolated crystalline **OMN**$^{+}$· cation-radical salt was extremely robust, remaining unchanged even at ambient temperatures for prolonged periods if protected from moisture.

X-ray crystallography established that **OMN**$^{+}$· cation−radicals and SbCl$_6^{-}$ anions cocrystallized in a 1:1 ratio, indicating that the organic moieties exist as fully oxidized species (Figure 6). As expected, the steric encumbrance from the peripheral methyl groups prevented the dimerization of **OMN**$^{+}$· with its neutral counterpart and led instead to the formation of infinite stacks of alternating monomeric **OMN**$^{+}$· and SbCl$_6^{-}$ in the crystals. The solid-state UV−vis spectrum (diffuse reflectance in an alumina matrix) was identical to that in solution (complete lack of NIR absorption band), which confirmed that this additional NIR band cannot be observed when the positive charge is trapped on the cation−radical instead of being delocalized over two neighboring moieties. Precise data on the molecular structure of **OMN**$^{+}$· could unfortunately not be obtained due to a severe disorder in both **OMN**$^{+}$· and SbCl$_6^{-}$ moieties, which precluded any accurate measurement of the bond length changes between neutral **OMN** and its monomeric **OMN**$^{+}$· cation−radical.

**Unhindered 2,3,6,7-Tetramethylnaphthalene TMN.** The treatment of unhindered 2,3,6,7-tetramethylnaphthalene **TMN** with NO$^{+}$SbCl$_6^{-}$ under similar reaction conditions, in dichloromethane at −20 °C, yielded a pink-purple solution. The UV−vis spectral analysis showed an absorption band at $\lambda_{max}$ = 575 nm ($\epsilon_{575}$ = 6700 M$^{-1}$ cm$^{-1}$) as well as a very broad band at 1150 nm (see Figure 5). This spectrum was readily assigned to the dimeric **(TMN)**$_2^{+}$· cation−radical by a comparison with the reported absorption spectrum of parent (naphthalene)$_2^{+}$· cation−radical dimer.[3a] Moreover, ESR analysis of the pink solution reproduced the reported spectrum[2b] (see Table 3) with the hyperfine splitting $a_H$ = 2.8 G (4H) and 1.1 G (12H). [Note that the observed hyperfine splitting $a_H$ = 5.6 G (4H) of hindered monomeric **OMN**$^{+}$· cation−radical is twice the value of dimeric **(TMN)**$_2^{+}$· cation−

radical.] For comparison, the spectral (ESR and UV−vis) data for all the compounds used in this study are summarized in Table 3.
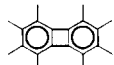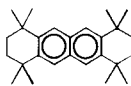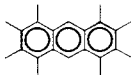
**C. Comparison of Paramagnetic Dimeric Cation−Radicals with Electron Donor/Acceptor (EDA) Complexes of Aromatic Donors.** The instantaneous formation of dimeric **(ArH)**$_2^{+}$· units when aromatic donors are exposed to their cation−radical **ArH**$^{+}$· as described in Figures 1 and 5 is highly reminiscent of the spontaneous complexation of aromatic donors with a variety of conventional electron acceptors.[12] In both cases, the intermolecular interaction of the aromatic donor is with an electron-poor species which is characterized by the immediate appearance of new spectral bands in the vis-NIR region that have been separately characterized as *charge-resonance* absorption in the case of dimeric cation−radicals (paramagnetic) and *charge-transfer* absorption for electron donor/acceptor (EDA) complexes (diamagnetic). The parallel is further strengthened by the structural similarity of the associated species, the cationic dimer and the electron donor/acceptor complex, both consisting of face-to-face bindings within tight van der Waals contacts.[23] The structural requirements of the latter is manifested by the susceptibility to steric effects, both charge-resonance and charge-transfer absorption bands disappearing when the intermolecular contacts become too weak or nonexistent because of steric hindrance (see Figure 5 and Rathore et al.,[13] respectively).

(21) (a) Gschwind, R.; Haselbach, E. *Helv. Chim. Acta* **1979**, *62*, 941. (b) Tsuchida, A.; Tsujii, Y.; Ohoka, M.; Yamamoto, M. *J. Phys. Chem.* **1991**, *95*, 5797.

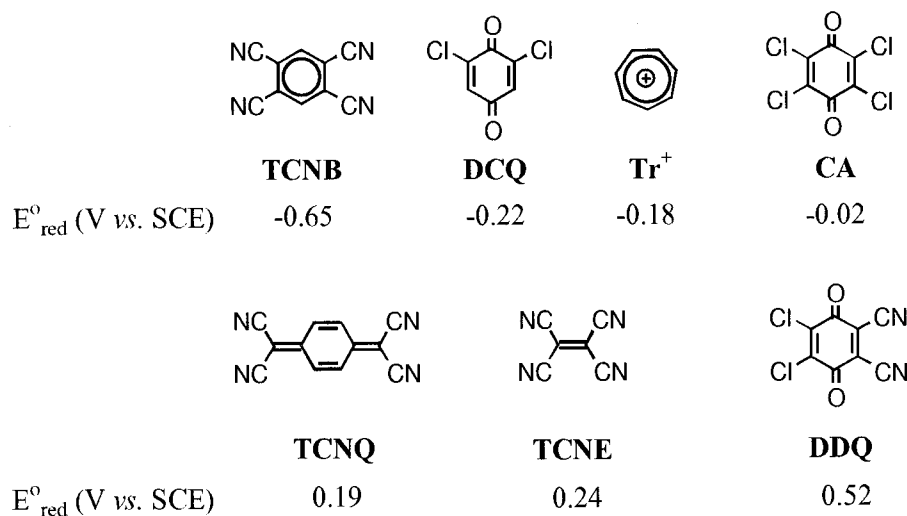(22) Sebastiano, R.; Korp, J. D.; Kochi, J. K. *J. Chem. Soc., Chem. Commun.* **1991**, 1481.

(23) For example, the single-crystal structure analysis of [**OMB**, **TCNQ**] charge-transfer complex (see Experimental Section) showed that the donor **OMB** and the acceptor **TCNQ** moieties are associated in pairs with a short interplanar contact of 3.14 Å. Moreover, both **OMB** and **TCNQ** molecules in the crystalline charge-transfer complex show considerable bond length reorganization in comparison to their respective neutral precursors, in accord with the degree of charge transfer from **OMB** to **TCNQ**. [The details of these results will be published in a following paper.]

**Table 3. Intermolecular π-dimers (ArH)$_2$⁺• of Stable Aromatic Cation—Radicals ArH⁺•**

| Donor (ArH) | | E°$_{ox}$ (V vs.SCE) | Monomer ArH⁺• | | Dimer (ArH)$_2$⁺• | | |
|---|---|---|---|---|---|---|---|
| | | | λ$_{max}$ (nm) | ESR[b] a$_H$(G) | UV-vis λ$_{max}$ (nm) | IR λ$_{max}$ (nm) | ESR[b] a$_H$(G) |
| **OMB** | | 0.80 | 600, 550 [a] | 4.5(12H) | 570 | 1850 | 2.3(12H) |
| **NAP** | | 1.73 [c] | 670, 610 [d] 530, 390 | e | 575 [f] | 1050 [f] | 2.77(8H) [g] 1.03(8H) |
| **TMN** | | 1.40 | 675, 616 [d] 510, 396 | e | 560 | 1150 | 2.9(4H) [h] |
| **OMN** | | 1.34 | 672, 616 [a] 503, 396 | 5.6(4H) | i | i | i |
| **OMA** | | 0.88 | 379, 447 [a] 477, 912 | 5.45 (2H) [j] 3.34 (12H) 1.67 (12H) | 400, 447 477, 912 | 2500 | e |

[a] Cation—radicals generated in dichloromethane from either NO⁺SbCl$_6$⁻, EtO⁺SbCl$_6$⁻,[11] or CA/CH$_3$SO$_3$H.[20] [b] Hyperfine coupling constants verified by ESR simulation.[15] [c] Irreversible peak potentials at scan rate $v = 0.5$ V s⁻¹. [d] See ref 21. [e] Not available. [f] Taken from ref 3a. [g] Taken from ref 2a. [h] Taken from ref 2b. [i] Does not form a dimer cation—radical even at −90 °C in the presence of high concentrations of neutral donor. [j] Taken from ref 21.

**Chart 2**

|  | **TCNB** | **DCQ** | **Tr⁺** | **CA** |
|---|---|---|---|---|
| E°$_{red}$ (V *vs.* SCE) | -0.65 | -0.22 | -0.18 | -0.02 |

|  | **TCNQ** | **TCNE** | **DDQ** |
|---|---|---|---|
| E°$_{red}$ (V *vs.* SCE) | 0.19 | 0.24 | 0.52 |

Despite the common features that the charge-resonance and charge-transfer bands share, it is not clear how they are related and what the actual differences are.

To quantify the qualitative resemblance between dimeric cation—radicals and EDA complexes, we consider in Chart 2 a series of traditionally electron-poor (diamagnetic) partners that are structurally diverse and with varying electron-accepting properties as measured by their reduction potentials ($E°_{red}$).[24] The spectral maxima of the charge-transfer absorption bands ($λ_{CT}$) with the three aromatic donors especially pertinent to this study,

viz., hexamethylbenzene (**HMB**), octamethylbiphenylene (**OMB**), and naphthalene (**NAP**) are listed in Table 4. For direct comparison, the charge-resonance bands ($λ_{CR}$) of the corresponding aromatic cation—radicals are also listed.

The results in Table 4 show that resonance absorption bands are consistently red-shifted by as much as 400—1000 nm relative to the charge-transfer bands. However, a careful consideration of the spectral data as *energy* changes considers the diamagnetic acceptors in Chart 1 and the aromatic cation—radicals only in terms of the reduction potentials. Accordingly, the energy gap ($E°_{ox} − E°_{red}$) between the HOMO of the aromatic donor ($E°_{ox}$) and the LUMO of the electron acceptor ($E°_{red}$) is plotted in Figure 7 against the energy ($hν_{CT}$ or $hν_{CR}$) of the spectral band in question. Note the dashed lines in Figures 7A—C are arbitrarily drawn with a unit slope. The unmistakable fit of the charge-resonance band to the

(24) The strength of the acceptors in Chart 2 can be evaluated by their reduction potentials. For **TCNB** and **TCNQ**, Mattes, S. L.; Farid, S. *Organic Photochemistry*; Padwa, A., Ed.; Dekker: New York, 1983; Vol. 6, p 238. For **DCQ**, **CA**, and **DDQ**, Mann, C. K.; Barnes, K. K. *Electrochemical Reactions in Nonaqueous Systems*; Dekker: New York, 1970. For **Tr⁺**, Wasielweski, M. R.; Breslow, R. *J. Am. Chem. Soc.* **1976**, *98*, 8, 4222. For **TCNE**, Rehm, D.; Weller, A. *Isr. J. Chem* **1970**, *8*, 259.

**Table 4. Absorption Maxima for Charge-transfer Complexes and Related Dimeric Cation–Radicals of Various Aromatic Donors in Dichloromethane at 20 °C**

| Acceptor | | **HMB** [a] $\lambda_{CT}$ (nm) $K_{DA}$ (M$^{-1}$) | **OMB** [b] $\lambda_{CT}$ (nm) $K_{DA}$ (M$^{-1}$) | **NAP** [c] $\lambda_{CT}$ (nm) $K_{DA}$ (M$^{-1}$) |
|---|---|---|---|---|
| **TCNB** | NC–⬡–CN / NC–⬡–CN | 423 (5.3) | 622 [f] | 397 (2.0) |
| **DCQ** | Cl–quinone–Cl | 462 (1.74) | 712 (4.5) | 425 [f] |
| **Tr$^+$** | ⬡$^+$ | 440 0.54 | 693 [f] | 425 (0.51) |
| **CA** | Cl$_4$-quinone | 520 (2.8) | 822 (14.4) | 480 (1.1) |
| **TCNQ** | NC/NC=⬡=CN/CN | 590 (13.5) | 870 (441) | 540 (0.63) |
| **TCNE** | NC/NC–C=C–CN/CN | 544 (15.3) | 880 [f] | 550 [f] |
| **DDQ** | NC/NC–quinone–Cl/Cl | 620 (100) | 880 (1100) | 615 (5.1) |
| **ArH$^{+\bullet}$** | | 1350 [d] | 1850 [d] (350) | 1050 [d] (685) |

[a] $E^0_{ox}$ = 1.62 V vs SCE. [b] $E^0_{ox}$ = 0.80 V vs SCE. [c] $E^0_{ox}$ = 1.73 V vs SCE. [d] Charge-resonance band for dimeric species (ArH)$_2^{+\bullet}$, see Table 1.
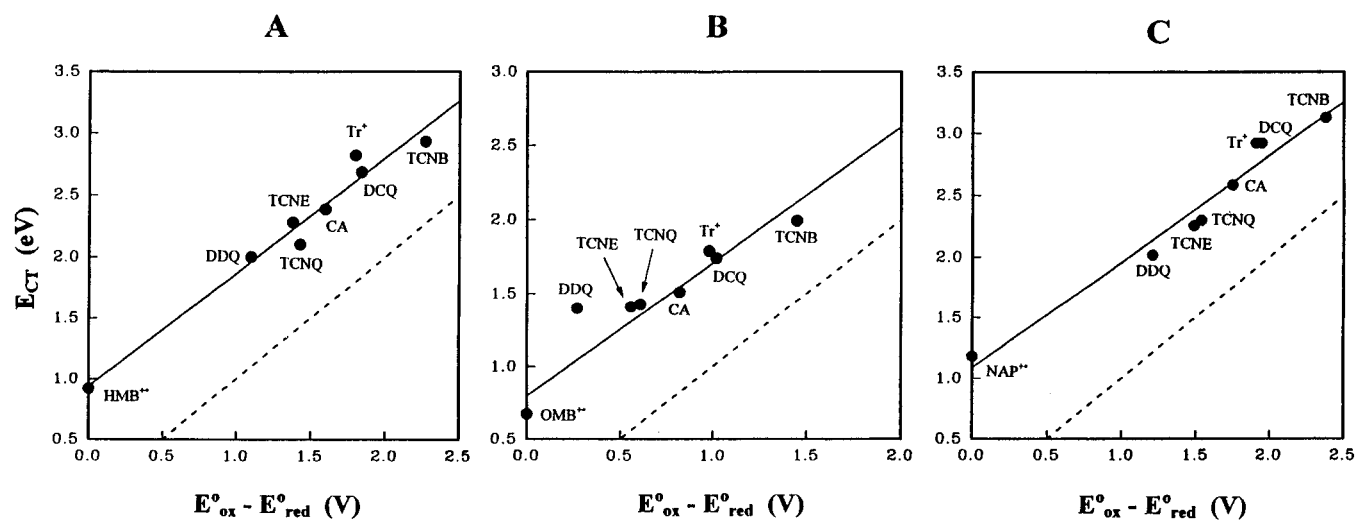


**Figure 7.** Mulliken plots for EDA complexes of (A) hexamethylbenzene **HMB**, (B) octamethylbiphenylene **OMB**, and (C) naphthalene **NAP** with various electron acceptors identified in Table 4. The solid lines represent the least-squares fit of the data. For comparison, the dashed lines are arbitrarily drawn with unit slope.

Mulliken correlation of the charge-transfer band is demonstrated in Figure 7 by the precise inclusion (within experimental error) of the points for all three cation–radicals **HMB$^{+\bullet}$**, **OMB$^{+\bullet}$**, and **NAP$^{+\bullet}$**. [Note that in dimeric cation–radicals the redox potentials of the electron acceptor **ArH$^{+\bullet}$** and the donor **ArH** are identical.] The spectral results thus indicate that the charge-transfer phenomenon between an aromatic donor and its cation–radical may be quantitatively viewed in the same basic terms as classical charge-transfer according to

Mulliken theory[12] despite the large red-shift in the spectral data to the NIR region.

Our next step is to compare the formation constants of common EDA ($\pi$,$\pi$)-complexes with the dimerization constants for various dimeric cation−radicals $(\mathbf{ArH})_2^{+\bullet}$. The values for the formation of EDA complexes with tetracyanobenzene (**TCNB**), tropylium cation ($\mathbf{Tr}^+$), chloranil (**CA**), dichlorobenzoquinone (**DCQ**), etc., lie in the range from 1 to 20 $M^{-1}$ whereas for dichlorodicyanobenzoquinone (**DDQ**) they range from 20 to 1200.[13,14] As for the cation-radical dimers, we have established previously the dimerization constant for the formation of $(\mathbf{OMB})_2^{+\bullet}$ to be 350 $M^{-1}$. In addition, the values for the formation of the cation−radical dimers of hexamethylbenzene, naphthalene $(\mathbf{NAP})_2^{+\bullet}$ ($K_{\text{dimer}} = 685$ $M^{-1}$ at $-15$ °C), 2,6-dimethylnaphthalene $(\mathbf{Me\text{-}NAP})_2^{+\bullet}$ ($K_{\text{dimer}} = 490$ $M^{-1}$ at $-10$ °C), and pyrene $(\mathbf{PYR})_2^{+\bullet}$ ($K_{\text{dimer}} = 510$ $M^{-1}$ at 20 °C) are known from the literature.[4a] It appears that the dimerization constants for dimeric cation−radical of aromatics all lie in the same range as the formation constant of EDA complexes of aromatic donors with **DDQ**.

In dimeric cation−radicals, the redox potentials of both donor **ArH** and acceptor $\mathbf{ArH}^{+\bullet}$ moieties are identical, which implies that the driving force for the dimerization is zero (not including the interaction energy). In EDA complexes of aromatic donors, the redox potential difference between the acceptor **A** and the donor **ArH** substrate is generally high. The exception is **DDQ**, which possesses the highest reduction potential relative to other common electron acceptors, and thus the driving force for the formation of EDA complexes with **DDQ** tends to be minimal and leads to high formation constants approaching that of mixed-valence aromatic dimeric cation−radicals.

## Summary and Conclusion

The close cofacial approach ($d \sim 3.4$ Å) of octamethylbiphenylene cation−radical to its neutral counterpart leads to strong electronic interactions between the two moieties which results in charge-resonance (CR) transitions in the electronic (NIR) absorption spectrum. Since the electron transfer driving force in such mixed-valence systems is zero, the position of the charge-resonance band is merely determined by the reorganization energy ($\lambda$) involved in the transformation from cation−radical to neutral molecule and the interaction energy. The comparison of the X-ray structures of monomeric and dimeric cation−radical leads to the conclusion that this charge-resonance results in an even delocalization of the positive charge over two donor molecules[19] as established by the analysis of the changes in bond lengths (Table 2) and the ESR data in Table 3.

The effect of steric encumbrance on the charge-resonance processes has been established by the utilization of the hindered naphthalene derivative **OMN** and its unhindered analogue **TMN**. Once oxidized, the sterically hindered $\mathbf{OMN}^{+\bullet}$ cation−radical remains singularly isolated (as demonstrated by X-ray crystallography) and shows no charge-resonance absorption in the UV−vis−NIR spectrum. By contrast, the unhindered relative **TMN** readily shows upon oxidation a new low-energy absorption band symptomatic of the formation of dimeric $(\mathbf{TMN})_2^{+\bullet}$ units.

Such a behavior is highly reminiscent of the sensitivity of electron donor/acceptor (EDA) complexes to steric

hindrance as reported previously,[13] and it indicates that similarities exist between the structure−property relationships of EDA complexes of aromatic compounds and those of their dimeric cation−radicals.[23] Most importantly, the charge-resonance absorption bands of the monomeric cation−radical species of various aromatic donors such as naphthalene, hexamethylbenzene, and octamethylbiphenylene are precisely included into the Mulliken plots of the charge-transfer data obtained with the EDA complexes of these arenes with common electron acceptors. This result suggests that mixed-valence dimeric cation−radicals represent a particular class of EDA complexes in which the charge transfer is actually a complete electron delocalization between both components.[19] Values for the formation constants of dimeric cation−radicals that are in the same range as those for strong complexes of aromatic donors with **DDQ** support this idea. For a more comprehensive comparison, we are currently examining hetero cation-radical $\pi$-complexes of an isolated (crystalline) cation−radical $\mathbf{ArH}_1^{+\bullet}$ salt with that of a different aromatic donor which show new charge-transfer (resonance) absorptions.[25]

## Experimental Section

**Materials.** The synthesis of octamethylbiphenylene,[26a] 2,3,6,7-tetramethylnaphthalene,[26b] 1,2,3,4,7,8,9,10-octahydro-1,1,4,4,7,7,10,10-octamethylnaphthacene,[20] and 1,2,3,4,5,6,7,8-octamethyanthracene[27] have been described previously. Triethyloxonium hexachloroantimonate (Aldrich) and nitrosonium hexachloroantimonate[28] salts were stored in a Vacuum Atmosphere HE-493 drybox kept free of oxygen. Dichloromethane (Mallinckrodt analytical reagent) was repeatedly stirred with fresh aliquots of concentrated sulfuric acid ($\sim$20 vol %) until the acid layer remained colorless. After separation, it was washed successively with water, aqueous sodium bicarbonate, water, and aqueous sodium chloride and dried over anhydrous calcium chloride. The dichloromethane was distilled twice from $P_2O_5$ under an argon atmosphere and stored in a Schlenk flask equipped with a Teflon valve fitted with Viton O-rings. The hexane and toluene were distilled from $P_2O_5$ under an argon atmosphere and then refluxed over calcium hydride ($\sim$12 h). After distillation from $CaH_2$, the solvents were stored in the Schlenk flasks under an argon atmosphere.

**Preparative Isolation of Monomeric Octamethylbiphenylene OMB Cation−Radical Salts Using $Et_3O^+SbCl_6^-$.** A 200-mL flask equipped with a Schlenk adapter was charged with triethyloxonium hexachloroantimonate (657 mg, 1.5 mmol), and a solution of **OMB** (266 mg, 1 mmol) in anhydrous dichloromethane (25 mL) was added under an argon atmosphere at $-20$ °C. The heterogeneous mixture immediately took on a blue coloration which intensified with time. The dark-colored mixture was stirred for 4 h to yield a blue solution of $\mathbf{OMB}^{+\bullet}$ [$\lambda_{\text{max}}$ (nm) = 600, 550 (sh), see Figure 1]. The dark-blue solution was cooled to $-50$ °C in a dry ice/acetone bath, and anhydrous toluene (100 mL) was added to precipitate the dissolved salt. The dark-blue precipitate was filtered under an argon atmosphere, washed with hexane (3 × 25 mL), and dried in vacuo. The highly pure cation−radical salt $\mathbf{OMB}^{+\bullet}$·$SbCl_6^-$ (vide infra) was obtained in essentially quantitative yield (530 mg, 0.88 mmol).

(25) A reviewer has suggested and we agree that the charge-resonance processes as described herein are amenable to Hush intervalence-band theory (e.g., Hush, N. S. *Prog. Inorg. Chem.* **1967**, *8*, 391) which we plan to present in later studies. (Sun, D. et al. Manuscripts in preparation.)

(26) (a) Hart, H.; Teuerstein, A.; Babin, M. A. *J. Am. Chem. Soc.* **1981**, *103*, 903. (b) Rieke, R. D.; White, K.; McBride, E. *J. Org. Chem.* **1973**, *38*, 1430.

(27) Welch, C. M.; Smith, H. A. *J. Am. Chem. Soc.* **1951**, *73*, 4391.

(28) (a) Sharp, D. W. A.; Thornley, J. *J. Chem. Soc.* **1963**, 3557. (b) Griffiths, J. E.; Sunder, W. A.; Falconer, W. E. *Spectrochim. Acta* **1975**, *31A*, 1207.

The purity of the isolated cation−radical salt **OMB**$^{+}$·SbCl$_6^{-}$ was determined by iodometric titration as follows.[29] A solution of **OMB**$^{+}$·SbCl$_6^{-}$ (60 mg, 0.01 M) in dichloromethane was added to a dichloromethane solution containing excess tetra-*n*-butylammonium iodide (1 mmol, 0.1 M) at 22 °C, under an argon atmosphere, to afford a dark-brown solution. The mixture was stirred for 5 min and was titrated (with rapid stirring) by a slow addition of a standard aqueous sodium thiosulfate solution (0.005 M) in the presence of starch as an internal indicator. On the basis of the thiosulfate solution consumed (59.4 mL), the purity of the cation−radical was determined to be >99%.

**Determination of Dimerization Constant ($K_{dimer}$) of OMB$^{+}$· Cation−Radical with Neutral OMB.** Typically, in a 1-cm square quartz cuvette (UV-cell) equipped with a sidearm and Schlenk adapter was placed a $1.2 \times 10^{-3}$ M solution of monomeric **OMB**$^{+}$· cation−radical in dichloromethane (with the aid of a hypodermic syringe) under an argon atmosphere. A 0.006 mM solution of neutral **OMB** in dichloromethane was added in increments (10 $\mu$L), and the absorbance changes were measured at the absorption maximum (1850 nm) as well as two other wavelengths close to the absorption maximum. The absorbance data were then evaluated with the aid of Benesi−Hildebrand correlation in eq 4.[14]

**Preparative Isolation of 1,1,4,4,7,7,10,10-Octamethyl-1,2,3,4,7,8,9,10-octahydronaphthacene OMN Cation−Radical Salt Using NO$^{+}$SbCl$_6^{-}$.** A 50-mL flask fitted with a Schlenk adapter was charged with nitrosonium salt (183 mg, 0.5 mmol), and a solution of **OMN** (172 mg, 0.5 mmol) in anhydrous dichloromethane (20 mL) was added under an argon atmosphere and ∼−10 °C. The nitric oxide produced (UV−vis spectral analysis of the gas revealed the characteristic absorbances of NO at $\lambda_{max}$ = 204, 214, and 226 nm)[30] was entrained by bubbling argon through the solution. The solution was stirred (while slowly bubbling argon) for 25 min to yield a deep-blue solution, which upon spectrophotometric analysis indicated the quantitative formation of **OMN**$^{+}$·SbCl$_6^{-}$. The blue solution was carefully layered with dry hexane (30 mL) and placed in a refrigerator (−23 °C). During the course of 2 days, dark-blue crystals of the cation−radical salt deposited (302 mg, 0.45 mmol).

**Construction of the Mulliken Plots of Hexamethylbenzene, Naphthalene, and Octamethylbiphenylene.** A series of absorption maxima ($\lambda_{CT}$) of new charge-transfer bands was obtained for each aromatic donor upon addition of the electron acceptors described in Chart 2 to a $10^{-3}$ M solution of the donor in a 1-cm square quartz cuvette (UV-cell) in dichloromethane at 20 °C. The values for the energy of the charge-transfer bands ($E_{CT} = hC/\lambda_{CT}$) were then plotted versus the difference $\Delta(E)$ between the oxidation potential of the donor **ArH** (**ArH** = **HMB**, **OMB**, or **NAP**) and the reduction potential of the acceptor (**A**) [$\Delta(E) = E^{o}_{ox}(\text{Ar}) - E^{o}_{red}(\text{A})$]. Note that $E_{CR}$ for (**ArH**$_2$)$^{+}$· was extracted from the absorption maxima of the charge-resonance bands (see Tables 1 and 3).

**Calculation of the Formation Constants of Donor/Acceptor Complexes.** A ∼1 mM solution of acceptor **A** in dichloromethane was placed in a 1-cm quartz cuvette (UV-cell), and a known amount of aromatic donor **ArH** was added in increments. The absorbance changes were measured at the absorption maxima of the new charge-transfer bands and treated according to the Benesi−Hildebrand correlation in eq 4.[14] The values of the dimerization constant and the extinction coefficient of the charge-transfer bands were readily extracted

from the slope [$K_{DA}\epsilon_{CT}$]$^{-1}$ and the intercept [$\epsilon_{CT}$]$^{-1}$ of the linear plot of [**A**]/$A_{CT}$ against [**ArH**]$^{-1}$.

**X-ray Crystallography.** The intensity data for all the compounds were collected with the aid of a Siemens SMART diffractometer equipped with a CCD detector using Mo−Kα radiation ($\lambda$ = 0.71073 Å), at −150 °C unless otherwise specified. The structures were solved by direct methods[31] and refined by full matrix least-squares procedure with IBM Pentium and SGI O$_2$ computers. [Note that the X-ray structure details of various compounds mentioned here are on deposit and can be obtained from Cambridge Crystallographic Data Center, U.K.]

**Monomeric 1,2,3,4,5,6,7,8-Octamethylbiphenylene Cation−Radical [(C$_{20}$H$_{24}$)$^{+}$ SbCl$_6^{-}$·CH$_2$Cl$_2$].** A dark-colored crystal with dimensions (0.16 × 0.14 × 0.10 mm) was selected for data collection. MW = 683.77, triclinic, space group $P$-1, $a$ = 9.6343(9), $b$ = 10.6007(9), and $c$ = 13.876(1) Å, α = 81.964(4)°, $\beta$ = 70.035(4)°, $\gamma$ = 80.276(4)°, $D_c$ = 1.737 g·cm$^{-3}$, $V$ = 1307.7(2) Å$^3$, $Z$ = 2. The total number of reflections measured were 16484 of which 11276 reflections were symmetrically nonequivalent. Final residuals were $R1$ = 0.0416 and w$R2$ = 0.0972 for 8080 reflections with $I > 2\sigma(I)$.

**Neutral 1,1,4,4,7,7,10,10-Octamethyl-1,2,3,4,7,8,9,10-octahydronaphthacene [C$_{26}$H$_{36}$].** A X-ray quality crystal (0.5 × 0.3 × 0.25 mm) of naphthalene derivative was obtained from toluene at ∼0 °C. MW = 348.55, monoclinic, space group $P2_1/n$, $a$ = 5.8991(1), $b$ = 22.0559(5), and $c$ = 8.3897(2) Å, $\beta$ = 108.880(1)°, $D_c$ = 1.121 g. cm$^{-3}$, $V$ = 1032.85(4) Å$^3$, $Z$ = 2. The total number of reflections measured were 12915, of which 4646 reflections were symmetrically nonequivalent. Final residuals were $R1$ = 0.0478 and w$R2$ = 0.1232 for 3926 reflections with $I > 2\sigma(I)$.

**Hindered 1,1,4,4,7,7,10,10-Octamethyl-1,2,3,4,7,8,9,10-octahydronaphthacene Cation−Radical [(C$_{26}$H$_{36}$)$^{+}$ SbCl$_6^{-}$].** A dark-blue crystal with dimensions (0.30 × 0.22 × 0.10 mm) was selected for data collection. MW = 683.00, orthorombic, space group $Cmca$, $a$ = 22.749(5), $b$ = 10.282(2), and $c$ = 12.513(3) Å, $D_c$ = 1.550 g. cm$^{-3}$, $V$ = 2927(1) Å$^3$, $Z$ = 4. The total number of reflections measured were 16399, of which 6845 reflections were symmetrically nonequivalent. Final residuals were $R1$ = 0.0725 and w$R2$ = 0.1399 for 3456 reflections with $I > 2\sigma(I)$.

**Dimeric 1,2,3,4,5,6,7,8-Octamethylanthracene Cation−Radical[19] [(C$_{22}$H$_{26}$)$_2^{+}$· SbCl$_6^{-}$].** A dark-colored crystal with dimensions (0.24 × 0.12 × 0.04 mm) was selected for data collection. MW = 915.31, triclinic, space group $P$-1, $a$ = 9.4063(3), $b$ = 9.4352(3), and $c$ = 11.8548(4) Å, α = 98.055(1)°, $\beta$ = 102.343(1)°, and $\gamma$ = 95.937(1)°, $D_c$ = 1.507 g. cm$^{-3}$, $V$ = 1007.93(6) Å$^3$, $Z$ = 1. The total number of reflections measured were 13714, of which 8677 reflections were symmetrically nonequivalent. Final residuals were $R1$ = 0.0255 and w$R2$ = 0.0597 for 7912 reflections with $I > 2\sigma(I)$. [The data collection was carried out also at −90 °C and at −30 °C, and the crystal data are available from Cambridge Crystallographic Data Center, see ref 19.]

(29) Rathore, R.; Kochi, J. K. *J. Org. Chem.* **1995**, *60*, 4399.

(30) Bosch, E.; Rathore, R.; Kochi, J. K. *J. Org. Chem.* **1994**, *59*, 2529.

(31) Sheldrick, G. M. *SHELXS-86, Program for Structure Solution*; University of Göttingen: Germany, 1986.